

## ARTICLE TYPE

## A short review on the pulsar magnetic inclination angles

Biao-Peng Li<sup>1,2,3</sup> | Zhi-Fu Gao<sup>\*1,2</sup><sup>1</sup>Xinjiang Astronomical Observatory,  
CAS,150, Science 1-Street, Urumqi,  
Xinjiang, 830011, China<sup>2</sup>Key Laboratory of Radio Astronomy,  
Chinese Academy of Sciences, West  
Beijing Road, Nanjing, 210008, China<sup>3</sup>University of Chinese Academy of  
Sciences, No.19, Yuquan Road, Beijing,  
100049, China

## Correspondence

\*Zhi-Fu Gao. Xinjiang Astronomical  
Observatory, CAS,150, Science 1-Street,  
Urumqi, Xinjiang, 830011, China.  
Email: zhifugao@xao.ac.cn

The inclination angle  $\chi$  between magnetic and rotation axes of pulsars is an important parameter in pulsar physics. The changes in the inclination angle of a pulsar would lead to observable effects, such as changes in the pulse beam width and braking index of the star. In this paper, we perform a short review on the evolution of pulsar's magnetic inclination angle, as well as the latest research progress. Using an alignment rotator model in vacuum, we investigate the magnetic inclination angle change rates for 12 high-braking index pulsars without glitch, whose timing observations are obtained using the Nanshan 25-m Radio Telescope at Xinjiang Astronomical Observatory. For our purpose, three representative pulsars J0157+6212, J1743-3150 and J1857+0526 are chosen and their rotation and inclination angle evolutions are further investigated. In the future, radio and X-ray polarimetric observations will provide more information about the inclination angles of pulsars, which could help us understand the origin of the variations in  $\chi$  of pulsars and shed light on the range of possibilities of pulsar magnetic field configuration. A continuous study of the pulsar inclination angle will provide an important window into additional physical processes at work in the young and highly magnetized pulsars.

## KEYWORDS:

pulsar, magnetic inclination angle, braking index, Nanshan 25-m Radio Telescope.

## 1 | INTRODUCTION AND MOTIVATION

Pulsars are highly magnetized and rapidly rotating neutron stars with rich emission phenomena, providing us an opportunity to explore physics under extreme conditions. A simplified model of pulsars is the classic vacuum magnetic dipole radiation where there is an angle between the magnetic axis and the axis of rotation (the inclination angle  $\chi$ ), which is an important parameter in pulsar physics. The variations in  $\chi$  of a pulsar would lead to observable effects, such as changes in the pulse beam width. The knowledge of initial angle  $\chi_0$  would provide valuable information about how pulsar magnetic fields are formed. Since the rotational energy loss rate and radio luminosity of pulsars depend on the inclination  $\chi$ , the values and time development of  $\chi$  have been described by various models (see e.g. (Barsukov, Polyakova, & Tsygan,

2009; Goldreich & Julian, 1969; Harding & Muslimov, 2002; Istomin & Shabanova, 2007; Kou, Tong, Xu, & Zhou, 2019; Ruderman & Sutherland, 1975)).

In general, the value of  $\chi$  of a pulsar can be independently determined by modeling of the gamma-ray or radio pulse profiles. Measurements of  $\chi$  were used to study possible alignment (or counter alignment) or decay of pulsar electromagnetic (EM) fields (Srinivasan, 1989). There are more than 200 pulsars with reported values of  $\chi$  by polarization measurements or other ways, and the angles distribute in a wide range of about  $5^\circ - 87^\circ$  (see e.g. (Tedila et al., 2022; ?; ?; ?)). With the exception of the Crab pulsar, it is difficult to accurately measure the variation of other pulsars' inclination angles, which involves many reasons, such as polarization position angle, dispersion measurement, pulse profile change and so on. The Crab pulsar is the only pulsar for which a change in  $\chi$  has been measured, at  $+(0.62 \pm 0.03)^\circ$  per century by observing the change in its radio pulse profile (Lyne et al.,

2013). However, the reason for the increase in  $\chi$  of this pulsar remains a mystery.

Since pulsars were discovered, to reveal the mysteries of radiation phenomena and rotational irregularity observed in pulsars, some theoretical models on the pulsar inclination angle have been proposed (see e.g. (Beskin & Nokhrina, 2007; Harding & Muslimov, 2002; Kou et al., 2019)). However, there are few reviews on the pulsar inclination angles and their evolutions, which makes it difficult to provide us with a more comprehensive understanding of the evolution mechanism of pulsar inclination angles. The variation of  $\chi$  could be associated with some observable phenomena in pulsars, such as slow glitches (Shabanova, 2005), profile change (S. Q. Wang et al., 2020; Wen et al., 2016, 2021), drifting subpulse (Yan et al., 2020, 2019; Yuen, 2019; Yuen & Melrose, 2014), pulsar braking indices that are different from the canonic dipole value (Ekşi et al., 2016; Lander & Jones, 2018; Tong & Kou, 2017). In view of this, we will perform a short review on the pulsar magnetic inclination angle, as well as their evolutions in this work.

This paper is organized as follows. In Section 2 we give a brief overview of the origin of variations in  $\chi$  of pulsars; In Section 3 we review the trends and forms of variations in  $\chi$  of pulsars; In Section 4 we review some observable effects in pulsars possibly related to variations in  $\chi$ ; In Section 5 we investigate the inclination angles and their evolutions for several pulsars observed by the Nanshan 25-m Radio Telescope within the framework of vacuum model. Section 6 gives a summary of this work.

## 2 | THE ORIGIN OF VARIATIONS IN INCLINATION ANGLE

The inclination angle  $\chi$  of a pulsar cannot remain constant throughout its lifetime. The variation in  $\chi$  either comes from inside or outside of the star, although variation mechanisms have not yet been understood. The angle  $\chi$  increases or decreases depending on the mechanism by which the pulsar loses energy.

### 2.1 | External origin

#### 2.1.1 | The vacuum model

If a pulsar's radiant energy is provided entirely by its rotational energy, pulsar rotating in vacuum will be slowed down by the radiation torques. Michel and Goldwire (1970) pointed out that there are two torques acting on the pulsar in the vacuum model: the spin-down torque that causes the rotational angular velocity to decrease with time and the alignment torque causing the magnetic inclination to evolve towards aligned

configuration,

$$I \frac{d\Omega}{dt} = -\frac{2}{3} \frac{M^2}{c^3} \Omega^3 \sin^2 \chi, \quad (1)$$

$$I \frac{d\chi}{dt} = -\frac{2}{3} \frac{M^2}{c^3} \Omega^2 \sin \chi \cos \chi, \quad (2)$$

where  $I$  is the moment of inertia,  $M$  the magnetic dipole moment,  $\Omega$  the rotational angular velocity, and  $c$  the speed of light. The alignment torque is an intrinsic component of the torque due to the magnetic dipole radiation. The vacuum model does not consider the presence of pulsar magnetosphere and is a very simplified pulsar model. Interestingly, due to its simplification, the vacuum model is still the most commonly used theoretical model in pulsar study.

#### 2.1.2 | The plasma-filled model

The pulsar magnetospheres are expected to be filled with a co-rotating plasma, which is formed by charged particles stripped from the surface of the star (Goldreich & Julian, 1969), and then accelerated by rotating-induced electric field along curved magnetic field lines to give an excess of electron-positron pair discharges, and only this configuration can keep the pulsar active. A change in the charge density and/or the current density will result in a variation in magnetospheric torque, thus  $\chi$  will change accordingly Spitkovsky (2006).

Philippov, Tchekhovskoy, and Li (2014) firstly gave a self-explanatory for the plasma effects by analysing the results of time-dependent force-free and magnetohydrodynamic (MHD) simulations of pulsar magnetosphere. Taking account into the plasma effects, the torque equations become

$$I \frac{d\Omega}{dt} = -\frac{2}{3} \frac{M^2}{c^3} \Omega^3 (1 + \sin^2 \chi), \quad (3)$$

$$I \frac{d\chi}{dt} = -\frac{2}{3} \frac{M^2}{c^3} \Omega^2 \sin \chi \cos \chi. \quad (4)$$

Obviously, both Eq.(1) and Eq.(3) have a common magnetic dipole braking torque in vacuum,

$$\mathbf{K}_{\text{dip}} = -\frac{2}{3} \frac{M^2}{c^3} \Omega^2 \sin^2 \chi, \quad (5)$$

which results in the loss of angular momentum of the pulsar. Philippov et al. (2014) also showed that pulsars evolve so as to minimize their spin-down luminosities: both the vacuum and plasma-filled pulsars evolve towards the aligned configuration. However, no pulsars with zero magnetic inclination angles have been observed, and the increasing in  $\chi$  of the Crab pulsar is difficult to be explained alone either in vacuum model or in plasma-filled model.

### 2.1.3 | The current-braking model

Oppositely, a current-braking pulsar will evolve towards the orthogonal configuration. According to Barsukov et al. (2009); Beskin, Gurevich, and Istomin (1993), there is a region in the pulsar magnetosphere, called the pulsar tube, which is formed by magnetic-field lines crossing the light cylinder. An electric current  $\mathbf{j}$  flows in the pulsar tube, and the current flowing from the star surface comes back in a narrow layer near the pulsar tube boundary due to conservation of charge. For these currents to be closed, a part of their paths must cross the magnetic field  $\mathbf{B}$ . Thus, the Lorentz force  $\mathbf{F} = [\mathbf{j} \times \mathbf{B}]/c$  acts on the polar-cap region, the associated torque acting on the crust is given by

$$\mathbf{K}_{\text{cur}} = -\frac{2}{3} \frac{M^3}{c^3} \Omega^2 \alpha \frac{\mathbf{M}}{M} \cos^2 \chi, \quad (6)$$

where  $\alpha$  is a parameter characterizing the magnitude of the electric current flowing through the pulsar tube. If a pulsar spends its energy for the generation and acceleration of plasma in the magnetosphere, and the star spins down due to the currents flowing in a magnetosphere and closing on the star surface, then the angle  $\chi$  approaches to  $90^\circ$ . This model gives an interesting relation of  $\nu \sin \chi = \text{const}$ , where  $\nu = \Omega/2\pi$  is the rotation frequency of the star. This relation requires that a pulsar stops spinning down, instead of rotates at a constant rotation frequency, when its inclination angle  $\chi$  increases to  $90^\circ$ . This appears to contradict observations.

### 2.1.4 | Complex braking models

A pulsar's secular spin-down could be simultaneously caused by several different energy loss mechanisms such as magnetic dipole radiation, particle wind, star-disk interaction, neutrino emission and gravitational radiation. The loss of rotational energy of a pulsar is accompanied by the change of  $\chi$ . Taking a complex braking model composed of the magnetic-dipole and current mechanisms for example, the total braking torque applied to a pulsar is  $\mathbf{K} = \mathbf{K}_{\text{dip}} + \mathbf{K}_{\text{cur}}$ , then the torque equations become (Barsukov et al., 2009)

$$I \frac{d\Omega}{dt} = -\frac{2}{3} \frac{M^2}{c^3} \Omega^3 (\sin^2 \chi + \alpha \cos^2 \chi), \quad (7)$$

$$I \frac{d\chi}{dt} = \frac{2}{3} \frac{M^2}{c^3} \Omega^2 (\alpha - 1) \sin \chi \cos \chi. \quad (8)$$

Here  $\alpha$  changes over time, if  $(\alpha - 1) > 0$ , then  $\dot{\chi} > 0$ , while  $(\alpha - 1) < 0$  and  $\dot{\chi} < 0$ .

## 2.2 | Internal origin

### 2.2.1 | Cooling and dipole-dipole interaction

The internal origin of the inclination angle change is related to the internal physics of neutron stars. Utilizing a

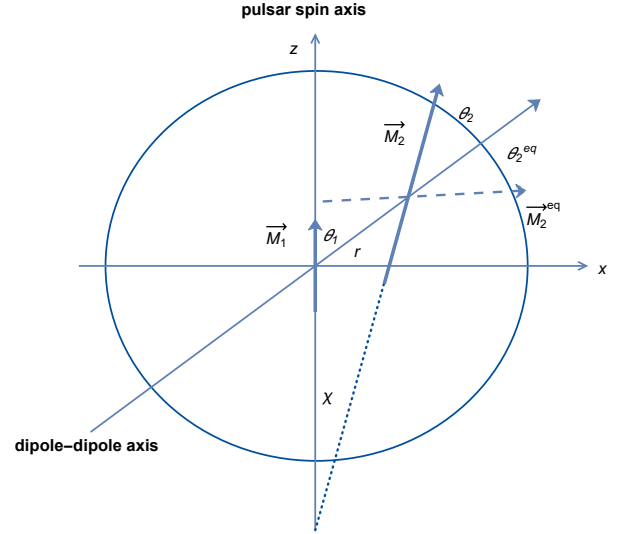


**FIGURE 1** The two-dipole system in the pulsar.  $\vec{M}_1$  is fixed and aligned with the spin axis  $z$ . The dipole-dipole axis  $r$  makes an angle  $\theta_1$  with  $z$ . The dashed line corresponds to  $\vec{M}_2$  in the equilibrium position. For more details see Hamil et al. (2016).

late-stage proto-neutron star model with a strong toroidal field, Lander and Jones (2018) found that the evolution of  $\chi$  is influenced by a combination of neutrino cooling, external electromagnetic torques, and internal dissipation. They show that, before the formation of the neutron star shell and before the neutron superfluidity and proton superconductivity internal dissipation will act to make  $\chi$  increase for star whose magnetic field-induced deformation is prolate. Their results show that a typical pulsar evolves into an near-orthogonal rotators and the millisecond magnetar with a small initial magnetic inclination and with a magnetic field greater than  $5 \times 10^{15}$  G evolves into near-aligned rotators.

Hamil et al. (2016) explored a double magnetic-dipole model of pulsars with a constant moment of inertia and magnetic dipole moment but variable magnetic inclination angle. In this model (Figure 1), there are two magnetic moments  $M_1$  and  $M_2$  inside the star. The former is generated by the rotation effect of a charged sphere, and the latter is generated by the magnetization of ferromagnetically ordered material. There will be mutual attraction or repulsion between  $M_1$  and  $M_2$ , resulting in a change in  $\chi$  for a pulsar. Whether an inclination angle increases or decreases and its change rate are dependent on a number of factors, such as the strength of the two magnetic moments, the minimum energy position.

It is proposed that the double magnetic-dipole model for pulsar inclination angle evolution may be most promising because it not only naturally explains the origin of magnetic fields in young and strongly magnetized pulsars, but also can account for some observable phenomena in pulsars, such as profile shifting, see the next section for details.

### 2.2.2 | Dissipation and precession

Let's consider a rotating pulsar in Cartesian coordinates. It is assumed that the principal symmetry axis of the pulsar is along the  $zz$  direction. Due to the centrifugal force effect, the pulsar should be oblate rotating along the  $zz$  axis. If the matter density distribution of the pulsar is asymmetric, the  $zz$  axis and the spin axis no longer coincide, and there is an angle between them, denoted as  $\beta$ . The value of  $\beta$  is affected by many factors, such as the rate of spin down and so on. As pulsar spins down, its rotational angular velocity also precessions around the  $zz$  axis, and the precession process affects the evolution of the inclination angle, including the magnitude and direction of evolution. Describing the above process in detail relies on the Euler's equations. It is worth emphasizing that in a pulsar precession cycle, the increase and decrease of the  $\chi$  appear alternately. When  $\chi$  is close to  $0^\circ$ , the change is very slow, but there will not be zero degrees. Similar change will occur in the inclination angle increase phase as  $\chi$  is close to  $90^\circ$ .

For example, considering the combined effect of magnetospheric current and magnetic dipole radiation Barsukov et al. (2009) gave the precession period that is

$$T_{\text{prec}} = \frac{2\pi}{\Omega_{\text{prec}}}, \quad \Omega_{\text{prec}} = -\frac{3}{5}\Omega \frac{M^2}{Rc^2 I} \cos \chi. \quad (9)$$

Dall'Osso and Perna (2017) studied the effect of viscous dissipation on the magnetic inclination distribution of young pulsars. The evolution equation for the inclination angle is

$$\tau_d \equiv \frac{E_{\text{prec}}}{|\dot{E}_{\text{diss}}|}, \quad \frac{d\chi}{dt} = \frac{\cos \chi}{\sin \chi \tau_d}, \quad (10)$$

where  $\tau_d$  is timescale for dissipation of the freebody precession,  $E_{\text{prec}}$  the precession energy and  $\dot{E}_{\text{prec}}$  the dissipation rate. They showed that the dissipation of precessional motions by bulk viscosity can naturally produce a bi-modal distribution of tilt angles, and proton superconductivity reduces the  $\beta$ -reaction rate, which causes the volumetric viscosity coefficient and the neutrino cooling rate to drop. Applied to the Crab pulsar, they found that there may be additional viscous processes, such as crust-core coupling via mutual friction in the superfluid core, which may affect the evolution of magnetic inclination angle over longer timescales.

Kraav, Vorontsov, and Barsukov (2017) considered the evolution of inclination angle and precession damping of radio pulsars and assumed that the neutron star consists of 3 "freely" rotating components: the crust and two core components, one of which contains pinned superfluid vortices. Within the framework of this model the star simultaneously can have glitch-like events combined with long-period precession (with periods  $10-10^4$  yrs). They found that the case of the small quantity of pinned superfluid vortices seems to be more consistent with observations.

## 3 | ON THE TRENDS AND FORMS OF THE INCLINATION ANGLE EVOLUTION

### 3.1 | The evolution trends

Increasing or decreasing of the  $\chi$  depends on the mechanism of a pulsar energy losses. There are three main variation trends for the pulsar inclination angle: near-aligned, near-orthogonal and oscillation trends.

1. For the first evolution trend, the inclination angle  $\chi$  decreases either when  $\chi$  is less than  $\pi/2$  and the rotation and magnetic axes are moving toward alignment, or when  $\chi$  is greater than  $\pi/2$  and the rotation and magnetic axes are counter-aligning.
2. For the second variation trend, although both internal dissipation and magnetospheric current models can increase the magnetic inclination angle, there is a difference. The internal dissipation that is temperature dependent dominate the early evolution of  $\chi$  in pulsars and gradually give way to electromagnetic torques as the neutrino cooling process progresses. The magnetospheric current model can cause a long-term increase in magnetic inclination angle.
3. For the third variation trend, similar to a simple pendulum, the inclination angle  $\chi$  of a pulsar is undergoing a long and permanent oscillation ( $\chi$  increases  $\rightarrow$  decreases  $\rightarrow$  increases ...). If a neutron star is triaxial ellipsoid, the angle  $\chi$  permanently oscillates around an equilibrium angle because of precession (Melatos, 2000). Also the oscillation trend has been predicted in the double magnetic-dipole model (Hamil et al., 2016).

### 3.2 | The evolution forms

There is also statistical evidence that the inclination angle of pulsars tends to achieve alignment in the long term (Young, Chan, Burman, and Blair (2010); ?).

Increasing inclination angle of Crab pulsar may require a further ingredient such as the presence of return currents in the magnetosphere or precession (Zanazzi & Lai, 2015). But an orthogonal rotator with plasma-filled force-free magnetosphere (Philippov et al., 2014) requires a much larger current than used in Beskin and Nokhrina (2007), so that the minimum spin-down energy losses correspond to that of an aligned rotator in the end.

According to vacuum model, a pulsar would stop spinning down when alignment is achieved in obvious contradiction with observations. It was suggested by Goldreich and Julian (1969) that the progress of alignment would be slowed down

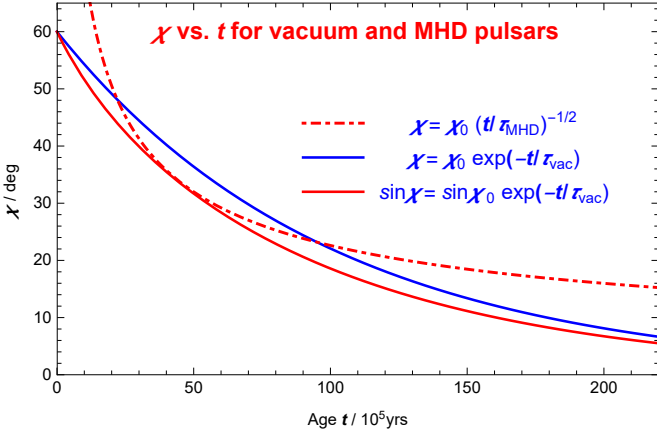


**FIGURE 2** Plot of magnetic inclination evolution comparison under vacuum model (solid lines) and plasma-filled magnetosphere model (dotted line). We arbitrarily choose parameters:  $\chi_0 = 60^\circ$ ;  $\tau_{\text{MHD}} = 1.42 \times 10^6 \text{ yrs}$ ;  $\tau_{\text{vac}} = 1.0 \times 10^7 \text{ yrs}$ .

by dissipative processes for a non-spherical pulsar. The magnetic inclination evolution in vacuum model is exponential,

$$\chi = \chi_0 \exp(-t/\tau_{\text{vac}}), \quad (11)$$

or

$$\sin \chi = \sin \chi_0 \exp(-t/\tau_{\text{vac}}), \quad (12)$$

where  $\tau_{\text{vac}}$  is the alignment time-scale of a vacuum pulsar. The sinusoidal form of Eq.(12) is convenient for calculating torques. After considering that plasma fills the magnetosphere, the evolution of  $\chi$  will be described by a relatively slow nonlinear form,

$$\chi = \chi_0 (t/\tau_{\text{MHD}})^{-1/2}, \quad (13)$$

where  $\tau_{\text{MHD}}$  is the MHD pulsar alignment time-scale.

In figure 2, we present a sketch that magnetic inclination angle evolves over time for the vacuum case and the MHD case. The inclination angle of MHD case diverges when time approaches zero. Although the plasma-filled magnetosphere model is relatively close to the realistic pulsar, its complex magnetospheric structure brings greater uncertainty. In this paper, we will choose simple vacuum model to study the inclination angle evolution for 12 pulsars from the Nshan observations, see the next section for details.

## 4 | ON THE OBSERVED EFFECT OF THE EVOLUTION OF INCLINATION ANGLE

### 4.1 | Slow glitches

Pulsar glitches are rare events of very short duration, shown as sudden jumps in rotational frequency (Yuan et al., 2017). The slow glitch was first coined when (Zou et al., 2004) tracked the

evolution of the frequency  $\nu$  and first-order frequency derivative  $\dot{\nu}$  of PSR B1822-09, with a continuous increase in  $\nu$  over several hundreds of days. This process corresponds to an impulsive decrease in the spin-down rate followed by an exponential increase to its pre-glitch value. Three slow glitches were observed in PSR B1822-09 by (Istomin & Shabanova, 2007). They explained the slow glitches well in a current-loss model in which the star's shape is rearranged during the inclination angle evolution because of the decelerating torque acting on the star. An orthogonal rotator fits the proposed model better than a co-axial rotator, which means that the inclination angle of the radio pulsar tends to  $90^\circ$  during its evolution.

### 4.2 | Radiation pulse profile

The inclination angle is an important parameter in the geometry of pulsar radiation that has a significant impact on changes in the pulse profile. ? reported that the core-component widths  $W_{\text{core}}$  depend only upon the pulsar period  $P$  and inclination angle  $\chi$ ,

$$W_{\text{core}} = 2.45^\circ P^{-1/2} / \sin \chi. \quad (14)$$

Maciesiak and Gil (2011) examined the validity of Eq.(14) by performing a statistical analysis of half-power pulse-widths of the core components in average pulsar profiles. Tedila et al. (2022) estimated the inclination angle of a long period pulsar (PSR J1900+4221) by using the Eq.(14) and obtained  $\chi = 7^\circ$ .

The nulling fraction (NF) was proposed in positive correlation with the age and the rotation period of a pulsar (Biggs, 1992). The evolution of the pulsar age is suggested in correlation with the inclination angle  $\chi$ . From consideration of energy loss through magnetic dipole radiation, the evolution of  $\chi$  is from large to small. However, consideration of the longitudinal current flow and the pair production in the magnetosphere Beskin, Gurevich, and Istomin (1988) suggests that the change of  $\chi$  is from small to large as a pulsar ages.

### 4.3 | Pulsar braking indice

A pulsar spins down due to electromagnetic radiation, particle winds, neutrino emission, or gravitational radiation. The long-term slowdown of the star follows a power-law form  $\tau_{\text{ext}} \propto \Omega^n$ , where  $\tau_{\text{ext}}$  is the external torque acting on the crust, and  $n$  is the braking index, which is an important quantity relating to the energy loss mechanism and determined by observations,

$$n = \frac{\nu \ddot{\nu}}{\dot{\nu}^2} = 2 - \frac{P \ddot{P}}{\dot{P}^2}, \quad (15)$$

where  $\ddot{\nu}$  is the second derivative of  $\nu$ , and  $\dot{\nu}$  is the derivative of  $\nu$ . It is generally assumed that the moment of inertia and the magnetic dipole moment are constant. If all the rotational energy

**TABLE 1** The spin frequencies, their derivatives, inclination angles and their change rates for pulsars with known braking indices. The superscripts 1 and 2 denote that the values of  $\dot{\chi}$  in Columns 8 and 9 are obtained using vacuum and MHD models, respectively. References: [1] Lyne et al. (1993); [2] Lyne et al. (1996); [3] Livingstone et al. (2007); [4] ?; [5] Roy et al. (2012); [6] Weltevrede et al. (2011); [7] Harding et al. (2008); [8] Dyks and Rudak (2003); [9] Watters et al. (2009); [10] Li et al. (2013); [11] Takata and Chang (2007); [12] Zhang and Cheng (2000); [13] Nikitina and Malov (2017); [14] Y. Wang et al. (2014); [15] Rookyard et al. (2015). Similar calculations of  $\dot{\chi}_1$  were performed by Tian (2018)

Pulsar	$\nu$ (s <sup>-1</sup> )	$\dot{\nu}$ (10 <sup>-11</sup> s <sup>-2</sup> )	$n$	Refs	$\chi$ (°)	Refs	$\dot{\chi}_1$ (°/100yr)	$\dot{\chi}_2$ (°/100yr)
Crab	30.2254	-38.6228	2.51(1)	[1]	45	[7]	0.558	1.412
					60	[8]	0.966	1.622
					70	[9]	8.486	1.877
Vela	11.2	-1.57	1.4(2)	[2]	62-68	[9]	0.38-0.51	0.82-0.98
					77-79	[9]	0.87-1.04	1.66-1.94
J1833-1034	16.1594	-5.2751	1.857(1)	[5]	70	[10]	0.926	1.727
J0540-6919	19.8345	-18.8384	2.140(9)	[3]	30	[11]	0.425	1.865
					50	[12]	0.877	2.16
J1734-3333	0.8552	-0.1667	0.9(2)	[4]	21	[13]	0.142	1.247
J1846-0258	3.0782	-6.7156	2.65(1)	[3]	10	[14]	0.121	4.12
J1119-6172	0.408	40.2	2.684(2)	[6]	21	[15]	0.108	0.949
J1513-5908	0.151	15.3	2.837(1)	[3]	60	[12]	0.255	0.595
					30	[15]	0.471	

loss of the pulsar is converted into magnetic dipole radiation, using Eq.(1), we get

$$n = 3 + 2 \frac{\nu}{\dot{\nu}} \frac{\dot{\chi}}{\tan \chi}. \quad (16)$$

Taking into account the plasma effect, equation (16) become

$$n = 3 + 2 \frac{\nu}{\dot{\nu}} \frac{\dot{\chi} \sin \chi \cos \chi}{1 + \sin^2 \chi}. \quad (17)$$

From Eqs(16) and (17),  $\dot{\nu} < 0$ , when  $\dot{\chi} > 0$ , there is  $n < 3$ , whereas  $\dot{\chi} < 0$ , then  $n > 3$ . Table 1 shows eight young pulsars with known braking indice. For comparison, we calculate the rate of change in magnetic inclination for the vacuum case and the MHD case by using Eq.(16) and Eq.(17), respectively.

For decades, despite their great success both vacuum and plasma-filled models should be combined with other radiation mechanisms such as gravitational wave, pulsar wind and internal dissipation to simulate the magnetosphere current, rotating, cooling and magnetic field evolution of pulsars.

A combination of gravitational wave and magnetic energy loss mechanisms radiation could give rise to a braking index  $3 < n < 5$  (de Araujo, Coelho, & Costa, 2016). To account for the observed braking indices, several other interpretations have been put forward, see Gao, Wang, Shan, Li, and Wang (2017) for a brief summary.

Table 1 does not include high-braking index PSR J1640-4631, whose value of  $\chi$  is predicted by the plasma-filled magnetosphere model Ekşi et al. (2016). Based on the estimated ages of their potentially associated supernova remnants (SNRs) and the timing parameters, Gao et al. (2016) measured the mean braking indices of eight magnetars with SNRs, and interpret the braking indices of  $n < 3$  within

a combination of MDR and wind-aided braking, while the larger braking indices of  $n > 3$  for other three magnetars are attributed to the decay of external braking torque, which might be caused by magnetic field decay.

Very recently, Yan, Gao, Yang, and Dong (2021) have applied a two-dipole model to two high- $n$  magnetars SGR 0501+4516 and IE 2259+586, and estimated their initial magnetic moments, initial inclination angles and average decrease rates of inclination angles. A comparisons with rotationally powered pulsars are presented. The decreasing magnetic inclination angle and narrow pulse width of a magnetar support its lack of radio emission.

## 5 | AN APPLICATION OF INCLINATION ANGLE EVOLUTION IN VACUUM MODEL

### 5.1 | Model and data

In this section, using an alignment rotator model in vacuum, we investigate the magnetic inclination angle change rates for 12 high-braking index pulsars without glitch, whose timing observations are obtained using the Nanshan 25-m Radio Telescope at Xinjiang Astronomical Observatory. Our data come from Dang et al. (2020). Although the plasma-filled magnetosphere model is relatively close to the realistic pulsar, its complex magnetospheric structure brings greater uncertainty. In this paper, we choose a relatively simple vacuum model to study the rotation evolution of pulsars. From Eqs(1) and (2),



**TABLE 2** Rotation and magnetic inclination angle evolution parameters ( $\nu$ ,  $\dot{\nu}$ ,  $\ddot{\nu}$ ,  $n$ ,  $\tau_c$ ,  $\chi$  and  $\dot{\chi}$ ) of 12 pulsars without glitches. The numbers in the parentheses represent the calculation errors. The data in Columns 1-6 and 10 are from Dang et al. (2020).

Pulsar name (J2000)	Epoch	$\nu$ (s <sup>-1</sup> )	$\dot{\nu}$ (10 <sup>-14</sup> s <sup>-2</sup> )	$\ddot{\nu}$ (10 <sup>-25</sup> s <sup>-3</sup> )	$n$	$\tau_c$ (10 <sup>5</sup> yrs)	$\chi$ (°)	$\dot{\chi}$ (°/100yrs)	Data Range (MJD)
J0157+6212	54594	0.425201	-3.414773(2)	0.136(7)	4.8(2)	1.974	46.5(1.5)	-0.0137(11)	52470–56719
J0614+2229	54595	2.985206	-5.27267(1)	53.8(6)	56.6(6)	8.978	11.93(6)	-0.0165(1)	52473–56718
J1739-2903	54598	3.097068	-7.554400(5)	0.13(2)	58.8(8)	6.501	11.72(8)	-0.0233(2)	52495–56702
J1743-3150	54599	0.414143	-2.071559(2)	0.067(5)	6.5(7)	3.171	37(8)	-0.012(1)	52495–56702
J1759-2922	54589	1.740942	-1.40276(1)	0.07(2)	33(19)	1.968	15.6(1.2)	-0.0056(26)	52496–56683
J1820-1346	54607	1.085232	-0.528865(3)	0.015(9)	60(34)	3.254	12(4)	-0.0047(12)	52496–56719
J1833-0338	54603	1.456193	-8.815136(2)	1.71(6)	34(1)	2.619	14.3(2)	-0.043(1)	52496–56719
J1857+0526	54619	2.857527	-5.658594(4)	0.19(1)	10(1)	8.008	28(2)	-0.0067(5)	52520–56718
J1902+0556	54288	1.339437	-2.309011(5)	0.09(2)	23(5)	9.199	18(2)	-0.0098(13)	52473–56103
J1916+0951	54587	3.700203	-3.448575(6)	0.10(2)	23(6)	1.702	17(3)	-0.0053(7)	52473–56700
J1918+1444	54644	0.846658	-15.20376(3)	6.39(8)	22.9(3)	8.831	17.6(1)	-0.102(1)	52569–56719
J2004+3137	54539	0.473643	-1.671669(2)	0.338(6)	62.6(8)	4.393	10.38(7)	-0.0348(3)	52488–56590

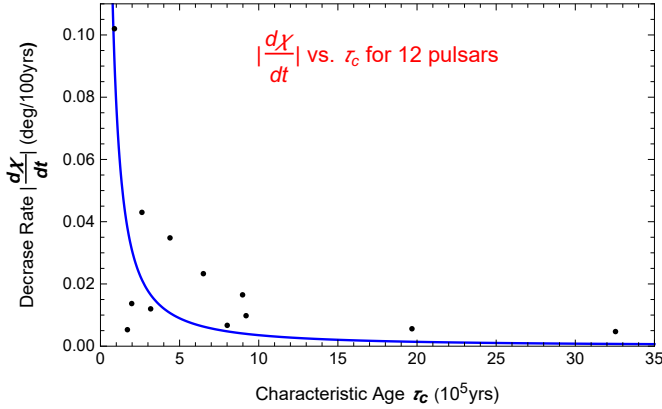


**FIGURE 3** The rate of change in inclination angle as a function of characteristic age.

we get

$$\dot{\chi} = \frac{\dot{\nu}}{\nu} \cot \chi. \quad (18)$$

From Eq.(18), one can get that the projection of the rotation angle frequency on the rotation axis is a constant,

$$\nu \cos \chi = \text{const}. \quad (19)$$

Since  $\nu$  always decreases, this requires a increasing  $\cos \chi$  and thus a decreasing  $\chi$ , ensuring the product of  $\nu \cos \chi$  is a constant. Combined with Eq.(16) we have

$$n = 3 + 2 \cot^2 \chi. \quad (20)$$

The second term on the right of Eq.(20) is positive, so  $n > 3$ . Then we get,

$$\cot \chi = \left( \frac{n-3}{2} \right)^{\frac{1}{2}}. \quad (21)$$

Dang et al. (2020) used the Nanshan 25-m radio telescope of Xinjiang Observatory to obtain the observation data of 87 pulsars for 12 years. These pulsars do not have glitches during the observation period. We selected 12 pulsars with the

braking indice  $3 < n < 100$ . Table 2 shows some parameters of these pulsars including inclination angles and their change rates calculated by using Eq.(18) and Eq.(21).

Then we use the data in Table 2 to fit the relationship between the change rates  $\dot{\chi}$  and the age  $\tau_c$ . Figure 3 shows the fitting results. In the fitting formula (22),  $\dot{\chi}$  is in units of deg/100yrs,  $\tau_c$  is in units of 10<sup>5</sup>yrs,

$$|\dot{\chi}| = a \times \tau_c^{-b}, \quad (22)$$

and the fitting parameters are  $a = 0.77(13)$  and  $b = 1.34(37)$ , where the numbers in the parentheses represent the errors. As can be seen from Figure 3, as pulsars spin down, the change rate of inclination angle  $\dot{\chi}$  declines continuously, the decline is faster in the early evolution and slower in the late evolution.

## 5.2 | Three representative pulsars

In pulsar observation, due to the influence of timing noise, the observed data will deviate from the actual situation, which will affect the measurement of certain parameters. Among these 12 sources, we believe that the source with a relatively large braking index has a large deviation from the actual one, and such a source needs to be further observed in the future. So we choose three pulsars J0157+6212, J1743-3150, J1857+0526 with  $3 < n < 10$  for further study.

Philippov et al. (2014) shows that the vacuum pulsars come into alignment exponentially. To explore the evolution of  $\nu$  over time, we use the data in Table 2 to obtain the constant of motion (Table 3) and assume that the evolution of  $\chi$  within the vacuum model is exponential as described by Eq.(11). The real ages of these three pulsars are estimated as  $t_a \approx -\frac{1}{n-1} \frac{\Omega}{\dot{\Omega}} = \frac{1}{n-1} \frac{P}{\dot{P}}$ . The spindown rate is then given as

$$\dot{\nu} = \frac{\sin \chi}{\cos^2 \chi} \dot{\chi} \text{const}. \quad (23)$$

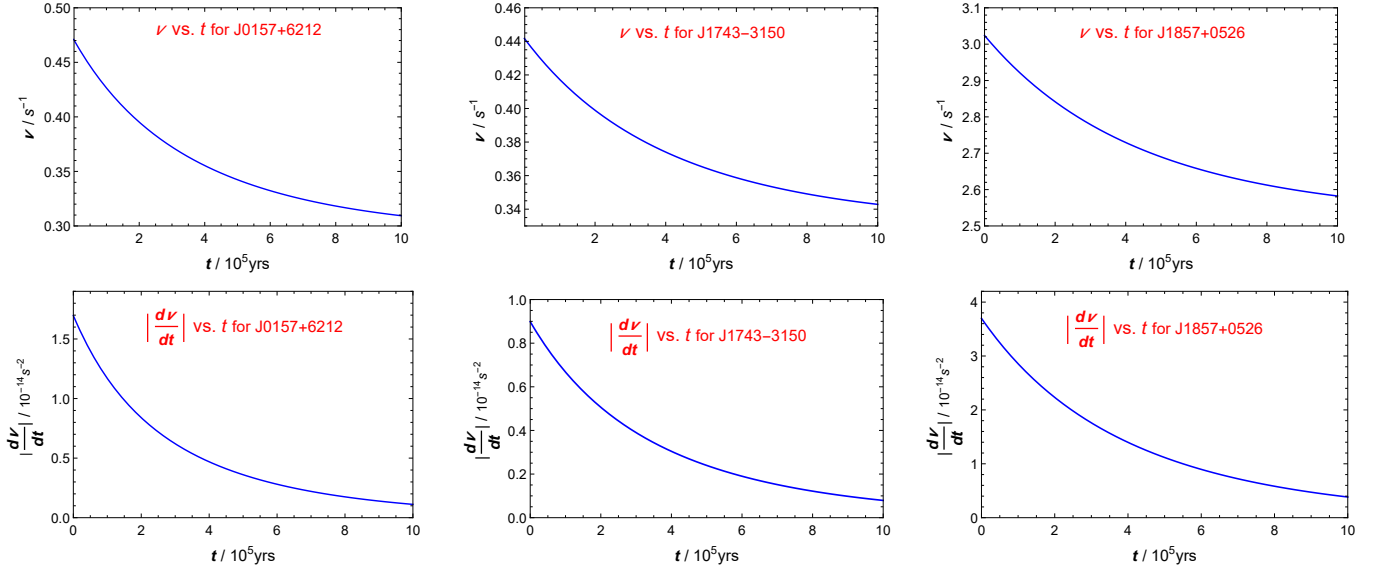


**FIGURE 4** Evolutions of  $\nu$  and  $\dot{\nu}$  over time  $t$  for J0157+6212, J1743-3150 and J1857+0526. The timescale of the evolution of magnetic inclination angle is taken as  $\tau_A = 10^6$  yrs for three sources.

**TABLE 3** Fitted parameters of three pulsars with braking index  $3 < n < 10$  under the vacuum model. The alignment time-scale is taken as  $10^6$  yrs.

Pulsar (J2000)	$t_a$ ( $10^5$ yrs)	$\chi_0$ ( $^\circ$ )	$\nu_0$ ( $s^{-1}$ )	const.
J0157+6212	1.039	51.60	0.47	0.293
J1743-3150	1.153	41.52	0.44	0.331
J1857+0526	1.779	33.45	3.02	2.523

Using Eqs(19) and (23), we make plots of  $\nu$  and  $\dot{\nu}$  over  $t$  for pulsars J0157+6212, J1743-3150 and J1857+0526, shown as in Figure 4. Table 3 lists the fitting parameters for the three pulsars including the actual age  $t_a$ , initial magnetic inclination  $\chi_0$  and the initial frequency  $\nu_0$ .

The possible relation between the evolution of the magnetic inclination and the rotation frequency has been investigated by Tian (2018). It is assumption that the various timing behavior unexpected by the magnetic dipole radiation is due to a secular change of  $\chi$ . Many other effects can also result in the same timing behavior such as the evolution of the magnetic field and an interaction between fall-back disk and magnetic field (Chen & Li, 2016). If we take into consideration these effects, the actual evolution of the magnetic inclination angles in Table 2 might differ very much from the values calculated.

## 6 | SUMMARY

In this paper, we have performed a short review on the the pulsar inclination angles, as well as their evolutions and given an application of inclination angle evolution in vacuum to 12 high- $n$  pulsars from the Nashan observation. In the future, it

is expected that polarization observations will give more values of the pulsars' inclination angles and their variations. We will combine observation phenomena to constrain the theoretical models, and explore the actual evolution process of these sources as much as possible.

## ACKNOWLEDGMENTS

This work was supported by Chinese National Science Foundation through No.12041304.

## REFERENCES

- Barsukov, D. P., Polyakova, P. I., & Tsygan, A. I. (2009), *Astronomy Reports*, 53(12), 1146-1154.
- Beskin, V. S., Gurevich, A. V., & Istomin, I. N. (1988), *Ap&SS*, 146(2), 205-281.
- Beskin, V. S., Gurevich, A. V., & Istomin, Y. N. 1993, *Physics of the pulsar magnetosphere*.
- Beskin, V. S., & Nokhrina, E. E. (2007), *Ap&SS*, 308, 569.
- Biggs, J. D. (1992), *ApJ*, 574.
- Chen, W.-C., & Li, X.-D. (2016), *MNRAS*, 455, 87.
- Dall'Osso, S., & Perna, R. (2017), *MNRAS*, 472, 2142.
- Dang, S. J., Yuan, J. P., Manchester, R. N., Li, L., Wang, N., et al. (2020), *ApJ*, 896, 140.
- de Araujo, J. C. N., Coelho, J. G., & Costa, C. A. (2016), *JCAP*, 2016, 023.
- Dyks, J., & Rudak, B. (2003), *ApJ*, 598(2), 1201.
- Ekşi, K. Y., Andaç, I. C., Çıkıntoğlu, S., Gügercinoğlu, E., Vahdat Motlagh, A., & Kızıltan, B. (2016), *ApJ*, 823, 34.
- Espinoza, C. M., Lyne, A. G., Kramer, M., Manchester, R. N., & Kaspi, V. M. (2011), *ApJ*, 741(1), L13.
- Gao, Z. F., Li, X. D., Wang, N., Yuan, J. P., Wang, P., Peng, Q. H., & Du, Y. J. (2016), *MNRAS*, 456, 55.



- Gao, Z.-F., Wang, N., Shan, H., Li, X.-D., & Wang, W. (2017), *ApJ*, 849, 19.
- Goldreich, P., & Julian, W. H. (1969), *ApJ*, 157, 869.
- Hamil, O., Stone, N. J., & Stone, J. R. (2016), *Phys. Rev. D*, 94, 063012.
- Harding, A. K., & Muslimov, A. G. (2002), *ApJ*, 568(2), 862.
- Harding, A. K., Stern, J. V., Dyks, J., & Frackowiak, M. (2008), *ApJ*, 680(2), 1378.
- Istomin, Y. N., & Shabanova, T. V. (2007), *Astronomy Reports*, 51, 119-125.
- Kou, F. F., Tong, H., Xu, R. X., & Zhou, X. (2019), *ApJ*, 876(2).
- Kraav, K. Y., Vorontsov, M. V., & Barsukov, D. P. (2017), *arXiv e-prints*, arXiv:1708.07505.
- Lander, S. K., & Jones, D. I. (2018), *MNRAS*, 481, 4169.
- Li, X., Jiang, Z. J., & Zhang, L. (2013), *ApJ*, 765(2).
- Livingstone, M. A., Kaspi, V. M., Gavriil, F. P., Manchester, R. N., Gotthelf, E. V. G., & Kuiper, L. (2007), *Ap&SS*, 308, 317.
- Lyne, A., Graham-Smith, F., Weltevrede, P., Jordan, C., Stappers, B., Bassa, C., & Kramer, M. (2013), *Sci*, 342, 598.
- Lyne, A. G., & Manchester, R. N. (1988), *MNRAS*, 234, 477.
- Lyne, A. G., Pritchard, R. S., & Graham Smith, F. (1993), *MNRAS*, 265, 1003.
- Lyne, A. G., Pritchard, R. S., Graham-Smith, F., & Camilo, F. (1996), *Nature*, 381(6582), 497.
- Maciesiak, K., & Gil, J. (2011), *MNRAS*, 417, 1444.
- Malov, I. F., & Nikitina, E. B. (2011), *Astronomy Reports*, 55(1), 19.
- Melatos, A. (2000), *MNRAS*, 313, 217.
- Michel, F. C., & Goldwire, J., H. C. (1970), *Astrophys. Lett.*, 5, 21.
- Nikitina, E. B., & Malov, I. F. (2017), *Astronomy Reports*, 61(7), 591.
- Philippov, A., Tchekhovskoy, A., & Li, J. G. (2014), *MNRAS*, 441, 1879.
- Rankin, J. M. (1990), *ApJ*, 352, 247.
- Rookyard, S. C., Weltevrede, P., & Johnston, S. (2015), *MNRAS*, 446(4), 3356.
- Roy, J., Gupta, Y., & Lewandowski, W. (2012), *MNRAS*, 424(3), 2213.
- Ruderman, M. A., & Sutherland, P. G. (1975), *ApJ*, 196, 51-72.
- Shabanova, T. V. (2005), *MNRAS*, 356, 1435.
- Spitkovsky, A. (2006), *ApJL*, 648, L51.
- Srinivasan, G. (1989), *A&A Rev.*, 1, 209.
- Takata, J., & Chang, H. K. (2007), *ApJ*, 670(1), 677.
- Tedila, H. M., Yuen, R., Wang, N., Yuan, J. P., Wen, Z. G., et al. (2022), *ApJ*, 929(2), 171.
- Tian, J. (2018), *New A*, 61, 100.
- Tong, H., & Kou, F. F. (2017), *ApJ*, 837, 117.
- Wang, N., Manchester, R. N., & Johnston, S. (2007), *MNRAS*, 377(3), 1383.
- Wang, S. Q., Hobbs, G., Wang, J. B., Manchester, R., Wang, N., et al. (2020), *ApJ*, 902(1), L13.
- Wang, Y., Ng, C. W., Takata, J., Leung, G. C. K., & Cheng, K. S. (2014), *MNRAS*, 445(1), 604.
- Watters, K. P., Romani, R. W., Weltevrede, P., & Johnston, S. (2009), *ApJ*, 695(2), 1289.
- Weltevrede, P., Johnston, S., & Espinoza, C. M. (2011), *MNRAS*, 411(3), 1917.
- Wen, Z. G., Wang, N., Yuan, J. P., Yan, W. M., Manchester, R. N., Yuen, R., & Gajjar, V. (2016), *A&A*, 592, A127.
- Wen, Z. G., Yuen, R., Wang, N., Tu, Z. Y., Yan, Z., et al. (2021), *ApJ*, 918(2), 57.
- Yan, F.-Z., Gao, Z.-F., Yang, W.-S., & Dong, A.-J. (2021), *AN*, 342, 249.
- Yan, W. M., Manchester, R. N., Wang, N., Wen, Z. G., Yuan, J. P., Lee, K. J., & Chen, J. L. (2020), *MNRAS*, 491(4), 4634.
- Yan, W. M., Manchester, R. N., Wang, N., Yuan, J. P., Wen, Z. G., & Lee, K. J. (2019), *MNRAS*, 485(3), 3241.
- Young, M. D. T., Chan, L. S., Burman, R. R., & Blair, D. G. (2010), *MNRAS*, 402(2), 1317.
- Yuan, J. P., Manchester, R. N., Wang, N., Wang, J. B., Zhou, X., Yan, W. M., & Liu, Z. Y. (2017), *MNRAS*, 466(1), 1234.
- Yuen, R. (2019), *MNRAS*, 486(2), 2011.
- Yuen, R., & Melrose, D. B. (2014), *PASA*, 31, e039.
- Zanazzi, J. J., & Lai, D. (2015), *MNRAS*, 451, 695.
- Zhang, L., & Cheng, K. S. (2000), *A&A*, 363, 575.
- Zou, W. Z., Wang, N., Wang, H. X., Manchester, R. N., Wu, X. J., & Zhang, J. (2004), *MNRAS*, 354, 811.